

Analysis of Information-Theoretic Initial Sensor Search Method for Space Situation Awareness

Koki Ho ¹

Georgia Institute of Technology, Atlanta, GA, 30332

Ryne Beeson ²

University of Illinois at Urbana-Champaign, Urbana, IL, 61801

Kento Tomita ³ and Onalli Gunasekara ⁴

Georgia Institute of Technology, Atlanta, GA, 30332

Andrew J. Sinclair ⁵

Air Force Research Laboratory, Albuquerque, NM 87117

I. Introduction

Over the years, the number of resident space objects has grown dramatically, and thus there is a growing need for characterizing the environment and potential threats in space to ensure safe space activities. To this end, the technologies to manage sensors to detect, identify, and predict orbiting small objects has become critical for space situational awareness (SSA) [1]. A large body of literature approached this sensor management problem by focusing on the assignment of sensors to objects [2–8]. These investigations have generally focused on the *global SSA problem*, with a goal to answer the question: given a network of sensors and prior probability distributions for the entire population of space objects, which sensors should be tasked to observe which objects?

Distinct from global SSA problems, another class of problems is related to a spacecraft's ability to maintain awareness of its own local environment using onboard sensors and being provided no or little cueing information. This class of problems can be referred to as *local SSA*. A motivating example is a single spacecraft with an angles-only sensor that has been provided limited cueing information on a single space object. The cueing information takes the form of a description of the probability density function of the object's orbit. The problem at hand is to task the spacecraft's sensor to search for the object. Under the typical assumptions of global SSA tasking methods, a single sensor and a single object is a trivial tasking problem. Under the assumptions in this Note, however, this problem is challenging because the projection of the object's orbit into the angles-only measurement space is assumed to be much larger than the sensor's field of view (FOV) [9, 10]. This scenario is illustrated in Fig. 1. Many sensor measurements will result in no detection of the object. Whereas sensor-tasking methods for global SSA often neglect the information contained in

¹Assistant Professor, Daniel Guggenheim School of Aerospace Engineering, Atlanta, GA 30332, AIAA Member.

²Ph.D. Candidate, Department of Aerospace Engineering, Urbana, IL, 61801.

³Ph.D. Student, Daniel Guggenheim School of Aerospace Engineering, Atlanta, GA 30332.

⁴Ph.D. Student, Daniel Guggenheim School of Aerospace Engineering, Atlanta, GA 30332.

⁵Senior Aerospace Engineer, Space Vehicles Directorate, Kirtland AFB, Air Force Research Laboratory, Albuquerque, NM 87117.

no-detection measurements, initial-search methods must directly account for this information. Such an initial-search capability is critical for follow-up observation of newly detected objects, detection of maneuvering or perturbed objects, searching for debris after a break-up event, or reacquisition of catalog objects with large orbital uncertainties [9].

This initial search problem has its unique challenges [9, 11], which make existing methods inapplicable. One of such challenges is the extremely large and non-Gaussian uncertainties in the object's state (i.e., position). For the space-based close-proximity follow-up observation example, the lack of range observability by close-proximity angles-only observation with optical sensors [12–14] can result in highly non-Gaussian uncertainties of the object's orbit. In addition, since the sensors are not perfect, they can return false alarms or missed detections; our sensor steering strategy needs to take such sensor imperfectness into account as well. Furthermore, particularly for space applications, we need a real-time approach to efficiently steer the sensor to detect the object, without relying on computationally intensive optimization methods.

The most straightforward approach to this initial search problem is a maximum-probability approach [11, 15, 16]. This approach points the sensor at the most probable candidate direction to capture the object in the FOV. Although this approach can identify the object quickly if the sensor is perfect, the stochastic nature of the sensor performance also leads to a motivation to narrow down the probability distribution (i.e., reduce the uncertainties) of the object state as much as possible. This motivation does not necessarily align with the maximum-probability approach, because we often need to point the sensor at various different directions before we can be sufficiently confident about which direction the true object is located at. Along these lines, global SSA sensor-tasking research has focused on information-theoretic approaches.

With this motivation, this Note analyzes an information-theoretic metric and its approach for initial sensor search and compares its expected performance with the maximum-probability approach. This information-theoretic approach points the sensor at the candidate direction that provides the largest amount of information about the uncertainties of the object state. The Kullback-Leibler divergence between the prior and posterior distribution can be used to quantify the amount of gained information, including information gained from no-detection measurements [17]. To date, we do not have an

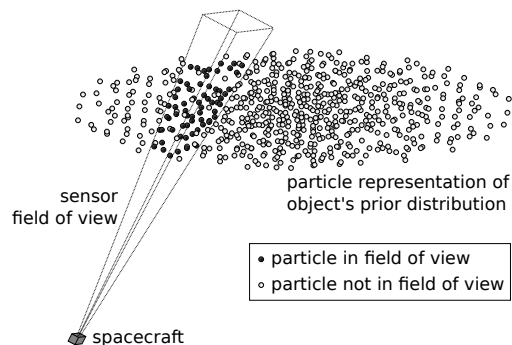


Fig. 1 Illustration of search scenario using a particle representation of the object's orbit.

analytical and systematic understanding of the difference between the maximum-probability and information-theoretic approaches for the initial search problem. This lack of understanding makes it challenging to provide a qualitative explanation about the role of the information-theoretic approach with respect to the maximum-probability approach in the context of initial sensor search. In response to this background, this Note formalizes the information-theoretic approach by providing a mathematical interpretation about the relationship between these two approaches and performing simulations to demonstrate their numerical performance. The main contribution of this Note is the derivation of a condition where the maximum-probability approach and information-theoretic approach are equivalent (i.e., where the maximum-probability approach is also optimizing the information-theoretic metric, or vice versa).

For analysis of the maximum-probability approach and the information-theoretic approach, we consider the same LEO-based single-sensor single-object search problem studied in the literature [17]. Following the convention in the past literature [11, 15–18], a binary sensor model is used where the sensor provides a binary detection measurement, i.e., either a detection or no detection measurement related to the presence of the object in the FOV; known nonzero probabilities for false alarms and missed detections are assigned. This simple model is expected to reflect the context of the initial sensor search, where our goal is to obtain observations of the object as soon as possible and as accurately as possible. In addition, we also follow the literature [11, 15–18] and use a particle representation for the object’s state probability distribution; these particles provide dual roles in approximating the distribution as well as discretizing the control search space defining how to steer the sensor at each observational time step.

II. Problem Statement

The goal of an initial sensor search problem is to reduce the uncertainty in the object’s state as we steer the sensor and make observations over time. In this Note, a particle representation is used for the object’s orbital probability distribution. The set of these particles is denoted by $\mathcal{X}(t) = \{x_t^1, x_t^2, \dots, x_t^n\}$, where $x_t^j \in \mathbb{R}^6$ for each time t and represents the position and velocity of the j -th particle. Each particle is considered to be a candidate orbit of the object with an assigned weight, corresponding to the probability of that particle being the object. The set of weights is denoted by $\mathcal{W}(t) = \{w_t^1, w_t^2, \dots, w_t^n\}$, such that $\sum_j w_t^j = 1$ for all time t . The particles are propagated over time with a two-body orbital dynamics. For instance, if $x_t = (r_t, v_t)$ are the position and velocity of a particle, then

$$\frac{d}{dt}r_t = v_t, \quad \frac{d}{dt}v_t = -\frac{\mu}{\|r_t\|^3}r_t, \quad (1)$$

where μ is the Earth’s gravitational constant. The evolution map associated with the particle dynamics is denoted by $\varphi : \mathbb{R}^6 \rightarrow \mathbb{R}^6$. Furthermore, x_t^* and x_t^s denote the state of the object and that of the observing spacecraft, respectively, both of which follow the same dynamics.

Our design variable is the direction to point the sensor at for each time step $(t_k)_{k \in \mathbb{N}}$. In the search algorithms

considered in this paper, we make use of the particle representation of the distribution to provide an appropriately reduced admissible control set. In particular, at time t_k , we define the control set \mathcal{U}_k to consist of the following unit vectors,

$$\mathcal{U}_k = \{u \mid u = (x_k^j - x_k^s) / \|x_k^j - x_k^s\|, j \in \{1, \dots, n\}\}. \quad (2)$$

That is, the admissible controls are the unit directions with origin at the observation spacecraft and in the direction of each of the particles $\{x_k^j\}$. Here, the subscript k indicates the time step t_k .

We consider the case of search for a single object with a single sensor. A binary sensor observation was used in the prior work [17–19] as a good representation for an initial search problem. In particular, given a control u_k , that defines the pointing direction at the k -th observation time, the sensor function $y_k = h(x_k^*, x_k^s, u_k)$ returns a 1 if a detection is made, and 0 if no detection is made. Typically, an angles-only sensor provides additional information when a detection is obtained, i.e., the actual angle values. Thus the binary model is a poor approximation if the probability of capturing the object in the FOV is high, such as during the later search stages or during precise tracking of an object. However, the binary model can approximate the initial search problem, where a large percentage of the measurements will be no detections. Given the observation y_k at time t_k , the set of weights $\mathcal{W}(t_k)$ associated with the particles $\mathcal{X}(t_k)$ can then be updated using the likelihood of detection and Bayes' rule:

$$w_k^j \propto p(y_k \mid \varphi(x_{k-1}^j); u_k) w_{k-1}^j \quad (3)$$

where $\varphi : \mathbb{R}^6 \rightarrow \mathbb{R}^6$ denotes the evolution map associated with the particle dynamics defined above. Denoting the FOV by $\text{FOV}(u_k)$, the likelihood of detection or no detection for the binary model is modeled as follows,

$$p(y_k = 1 \mid \varphi(x_{k-1}^j); u_k) = \begin{cases} p_{DDP} & \varphi(x_{k-1}^j) \in \text{FOV}(u_k) \\ p_{DDA} & \varphi(x_{k-1}^j) \notin \text{FOV}(u_k) \end{cases} \quad (4)$$

$$p(y_k = 0 \mid \varphi(x_{k-1}^j); u_k) = \begin{cases} p_{NDP} & \varphi(x_{k-1}^j) \in \text{FOV}(u_k) \\ p_{NDA} & \varphi(x_{k-1}^j) \notin \text{FOV}(u_k) \end{cases} \quad (5)$$

where p_{DDP} is probability of true detection, p_{DDA} probability of a false alarm (i.e., false positive), p_{NDA} probability of accurate no detection, and p_{NDP} probability of a missed detection (i.e., false negative). In the subscripts, the first letter indicates D (detection) or N (no detection), whereas the second letter indicates P (the object present in the FOV) or

A (the object absent in the FOV). It is assumed that $p_{DP}, p_{DA}, p_{NP}, p_{NA} \in (0, 1)$ and that $p_{DP} > p_{DA}$ and hence $p_{NP} < p_{NA}$; this relationship indicates that the probability of true detection is larger than the probability of a false alarm. Note that, by definition, the following relationships are true:

$$p_{DP} + p_{NP} = 1 \quad (6)$$

$$p_{DA} + p_{NA} = 1 \quad (7)$$

One source of false alarms that can be accounted for in p_{DA} is measurement correlation errors, i.e., when an object other than the intended object is detected. The particle representation is well suited to the binary sensor model. Whereas this type of non-differentiable sensor model cannot be accommodated in an extended Kalman filter, it is directly accommodated in the particle representation via the Bayes update in Eq. (3). Additionally, even if the prior distribution is Gaussian, the binary sensor model can result in a highly non-Gaussian posterior distribution. We refer the reader to Refs. [17–19] for further details of the binary sensor model.

III. Searching Algorithms

In this Note, we analyze two types of sensor steering algorithms, a maximum-probability one and an information-theoretic one, for searching and detecting the object as quickly and sufficiently often enough. Both algorithms are concerned with finding a control sequence (u_k) such that a specific objective function is maximized at each observation time (t_k) . We are interested in the comparison of the expected performance of these two algorithms. Both algorithms are here implemented in a greedy-in-time approach, i.e., planning the next measurement independently from the rest of the search campaign. The limitations of the greedy-in-time approach were studied for the multi-sensor/multi-object tasking problem in Ref. [8].

A. Maximum Probability Search Algorithm

The first approach, which is referred to as Maximum Probability Search Algorithm (MPSA) in this work, aims to choose a control u_k at observation time t_k from an admissible set \mathcal{U}_k , such that the (prior) probability that the object is in the FOV generated by u_k is maximized. Note that maximizing the probability that the object is in the FOV is equivalent to maximizing the probability of detection because of our assumption: $p_{DP} > p_{DA}$. Mathematically, this metric takes the following form,

$$u_k^o = \arg \max_{u \in \mathcal{U}_k} p_{k|k-1}(x_k^* \in \text{FOV}(u)), \quad (8)$$

where $\text{FOV}(u)$ is the FOV generated by u . With our previously-defined particle representation for uncertainties and weights, Eq. 8 reduces to the computable form

$$u_k^o = \arg \max_{u \in U_k} \sum_{j \in J(u)} w_{k-1}^j, \quad J(u) = \{j \mid j \in \{1, \dots, n\}, x_k^j \in \text{FOV}(u)\}. \quad (9)$$

This metric for MPSA (i.e., the sum of weights of the particles within the FOV) is denoted by W_u :

$$W_u = \sum_{j \in J(u)} w_{k-1}^j, \quad J(u) = \{j \mid j \in \{1, \dots, n\}, x_k^j \in \text{FOV}(u)\}. \quad (10)$$

B. Kullback-Liebler Search Algorithm

The second objective function is an information-theoretic approach, which chooses the control u_k such that the expectation of Kullback-Liebler (KL) divergence of the posterior from the prior distribution is maximized at time t_k . We refer to this approach as the KL Search Algorithm (KLSA). The mathematical definition of KL divergence for a distribution p from q is given by,

$$D_{KL}(p||q) = \int_{\mathcal{X}} p(dx) \ln \frac{dp}{dq}(x), \quad (11)$$

where dp/dq is the Radon-Nikodym derivative of p with respect to q . The optimal control from the admissible set \mathcal{U}_k , given by Eq. 2, is then defined as

$$u_k^o = \arg \max_{u \in U_k} \mathbb{E} [D_{KL}(p_{k|k}(x|y; u) || p_{k|k-1}(x|y))]. \quad (12)$$

With our previously-defined particle representation for uncertainties and weights, the KL divergence can be written as

$$\begin{aligned} & D_{KL}(p_{k|k}(x|y; u) || p_{k|k-1}(x|y)) \\ &= \sum_j p(\varphi(x_{k-1}^j) | y_k; u) \ln \frac{p(\varphi(x_{k-1}^j) | y_k; u)}{p(\varphi(x_{k-1}^j) | y_{k-1})} \\ &= \sum_j \frac{p(y_k | \varphi(x_{k-1}^j); u) w_{k-1}^j}{\sum_i p(y_k | \varphi(x_{k-1}^i); u) w_{k-1}^i} \ln \frac{p(y_k | \varphi(x_{k-1}^j); u) w_{k-1}^j}{\left(\sum_i p(y_k | \varphi(x_{k-1}^i); u) w_{k-1}^i \right) w_{k-1}^j} \\ &= \sum_j \frac{p(y_k | \varphi(x_{k-1}^j); u) w_{k-1}^j}{\sum_i p(y_k | \varphi(x_{k-1}^i); u) w_{k-1}^i} \ln \frac{p(y_k | \varphi(x_{k-1}^j); u)}{\sum_i p(y_k | \varphi(x_{k-1}^i); u) w_{k-1}^i} \end{aligned} \quad (13)$$

Acknowledging that in the binary model $Y = \{y\}$ is a singleton and either $y = 1$ or $y = 0$ (i.e. a detection or no detection), then expectation of Eq. 13 simplifies nicely to the tractable,

$$\begin{aligned} & \mathbb{E} [D_{KL}(p_{k|k}(x|Y; u) || p_{k|k-1}(x|Y))] \\ &= \sum_j p(y_k = 1 | \varphi(x_{k-1}^j); u) w_{k-1}^j \ln \frac{p(y_k = 1 | \varphi(x_{k-1}^j); u)}{\sum_i p(y_k = 1 | \varphi(x_{k-1}^i); u) w_{k-1}^i} \\ &+ \sum_j p(y_k = 0 | \varphi(x_{k-1}^j); u) w_{k-1}^j \ln \frac{p(y_k = 0 | \varphi(x_{k-1}^j); u)}{\sum_i p(y_k = 0 | \varphi(x_{k-1}^i); u) w_{k-1}^i}. \end{aligned} \quad (14)$$

This metric for KLSA (i.e., the expectation of KL divergence of the posterior from the prior distribution) is denoted by KL_u :

$$KL_u = \mathbb{E} [D_{KL}(p_{k|k}(x|y; u) || p_{k|k-1}(x|y))] . \quad (15)$$

Note that evaluation of Eq. (14) has higher computational cost than the simple summation of weights that is necessary for Eq.(9).

IV. Analysis

In this section, we compare the metrics for MPSA and KLSA (i.e., W_u and KL_u) and analyze their relationship. We start from the metric for KLSA for the binary sensor case. By substituting Eqs. 4-5 into Eq. 14, we obtain the following expression for KL_u :

$$\begin{aligned} KL_u &= \sum_{j \in J(u)} p_{DP} w_{k-1}^j \ln \frac{p_{DP}}{\sum_{i \in J(u)} p_{DP} w_{k-1}^i + \sum_{i \notin J(u)} p_{DA} w_{k-1}^i} \\ &+ \sum_{j \notin J(u)} p_{DA} w_{k-1}^j \ln \frac{p_{DA}}{\sum_{i \in J(u)} p_{DP} w_{k-1}^i + \sum_{i \notin J(u)} p_{DA} w_{k-1}^i} \\ &+ \sum_{j \in J(u)} p_{NP} w_{k-1}^j \ln \frac{p_{NP}}{\sum_{i \in J(u)} p_{NP} w_{k-1}^i + \sum_{i \notin J(u)} p_{NA} w_{k-1}^i} \\ &+ \sum_{j \notin J(u)} p_{NA} w_{k-1}^j \ln \frac{p_{NA}}{\sum_{i \in J(u)} p_{NP} w_{k-1}^i + \sum_{i \notin J(u)} p_{NA} w_{k-1}^i}, \end{aligned} \quad (16)$$

where

$$J(u) = \{j | j \in \{1, \dots, n\}, x_k^j \in \text{FOV}(u)\} \quad (17)$$

Noting that

$$\sum_{j \in J(u)} w_{k-1}^j = W_u \quad (18)$$

$$\sum_{j \notin J(u)} w_{k-1}^j = 1 - W_u \quad (19)$$

Eq.16 can be written as:

$$\begin{aligned} KL_u &= p_{DPP} W_u \ln \frac{p_{DPP}}{p_{DPP} W_u + p_{DA}(1 - W_u)} \\ &+ p_{DA}(1 - W_u) \ln \frac{p_{DA}}{p_{DPP} W_u + p_{DA}(1 - W_u)} \\ &+ p_{NPP} W_u \ln \frac{p_{NPP}}{p_{NPP} W_u + p_{NA}(1 - W_u)} \\ &+ p_{NA}(1 - W_u) \ln \frac{p_{NA}}{p_{NPP} W_u + p_{NA}(1 - W_u)}. \end{aligned} \quad (20)$$

Note that KL_u can be written as a function of W_u and constants, which allows us to analyze the behavior between the MPSA and KLSA. Moreover, we note that KL_u is a concave function of W_u because $p_{DPP} \neq p_{DA}$ and $p_{NPP} \neq p_{NA}$. Excluding the edge case, the maximum value of KL_u at $W_u = W^*$ can be obtained by solving:

$$\frac{dKL_u}{dW_u} = 0. \quad (21)$$

The analytical expression for the left side of Eq. 21 is

$$\begin{aligned} \frac{dKL_u}{dW_u} &= p_{DPP} \ln \frac{p_{DPP}}{p_{DPP} W_u + p_{DA}(1 - W_u)} - p_{DA} \ln \frac{p_{DA}}{p_{DPP} W_u + p_{DA}(1 - W_u)} - (p_{DPP} - p_{DA}) \\ &+ p_{NPP} \ln \frac{p_{NPP}}{p_{NPP} W_u + p_{NA}(1 - W_u)} - p_{NA} \ln \frac{p_{NA}}{p_{NPP} W_u + p_{NA}(1 - W_u)} - (p_{NPP} - p_{NA}) \end{aligned} \quad (22)$$

Leveraging Eqs. 6-7,

$$\begin{aligned} \frac{dKL_u}{dW_u} &= p_{DPP} \ln \frac{p_{DPP}}{p_{DPP} W_u + p_{DA}(1 - W_u)} - p_{DA} \ln \frac{p_{DA}}{p_{DPP} W_u + p_{DA}(1 - W_u)} \\ &+ p_{NPP} \ln \frac{p_{NPP}}{p_{NPP} W_u + p_{NA}(1 - W_u)} - p_{NA} \ln \frac{p_{NA}}{p_{NPP} W_u + p_{NA}(1 - W_u)} \end{aligned} \quad (23)$$

Using the above expression, the solution for Eq. 21 can be obtained using a standard numerical solver. Note that for the special case of $p_{DPP} = p_{NA}$, the solution is $W_u = W^* = 0.5$. Leveraging the fact that KL_u is a concave function of W_u , we can reach the following interpretation of this solution W^* :

- If the maximum W_u among all action candidates is smaller than W^* , then both the MPSA and KLSA approaches

would choose that same action (i.e., the one with the maximum W_u). This is the region where the maximum- W_u action matches the maximum- KL_u action.

- If the maximum W_u among all action candidates is larger than W^* , then the MPSA approach would choose that action with the maximum W_u , whereas the KLSA approach would instead choose an action that has W_u equals to W^* , or, if such an action candidate does not exist, the action that has W_u closest to W^* . This is the region where the maximum- W_u action does not match the maximum- KL_u action, because the latter is realized when $W_u = W^*$ (or $W_u \sim W^*$ if it does not exist), not by the maximum W_u .

At the beginning of the search campaign, the particle weights are equally distributed, and so the sum of particle weights in the FOV chosen by the MPSA may be a small value, i.e. less than W^* . This implies that the MPSA and KLSA will initially steer the sensor in the same direction. This result is significant because it shows that the MPSA is equivalent to the KLSA (i.e., the MPSA is also maximizing the KLSA objective) for the initial search problem, but with lower computational expense.

However, as the probability distribution is refined, the MPSA will reach a point in the search campaign where W_u is greater than W^* . From this point forward, the MPSA will continue pursuing a larger W_u , whereas the KLSA will "stall" there and continue taking the actions with W_u approximating W^* . For example, for the case with equal probabilities of missed detections and false alarms noted before, W^* equals 0.5; then, the KLSA will prefer to point the sensor in a direction whose FOV contains the object with a probability of 50%. This result can be intuitively understood as the direction that provides the maximum amount of information, as opposed to the directions with small (or large) values of W_u that would likely only confirm the expected result, i.e. absence (or presence) of the object in the FOV. Note that this most information-rich direction W^* depends on the values of p_{DP} and p_{NA} : e.g., if $p_{DP} = 0.7$ and $p_{NA} = 0.9$, then $W^* = 0.47$; if $p_{DP} = 0.9$ and $p_{NA} = 0.7$, then $W^* = 0.53$. Note that, in practice, during these later stages of the search, the binary sensor model considered in this Note will be a poor approximation of an optical sensor, and the tasking problem should be transitioned to algorithms built on higher-fidelity sensor models.

V. Simulations

To demonstrate the performance of the MPSA and KLSA approaches, we perform Monte Carlo simulations. In the simulations, the object's orbit and candidate orbits (i.e. particles) are selected from Gaussian distributions in the position and velocity components. The distribution parameters and other simulation parameters are shown in Table 1.

One of the key metrics of interest is the probability of the object being in the FOV, $P[\text{object}]$, defined as the fraction of the Monte Carlo samples having the object in the FOV at a given time. We plot the evolution of this metric over observation steps for each approach in Fig. 2. In this plot, initially, the MPSA and KLSA both experience an increase in $P[\text{object}]$ in a similar way; however, beyond the point of $P[\text{object}] > 0.5$, the $P[\text{object}]$ for the KLSA approach "stalls" around $P[\text{object}] \sim 0.5$, whereas that for the MPSA approach continues to grow beyond 0.5. This interesting trend

can be explained by the aforementioned mathematical analysis result that the information-theoretic KLSA approach prefers to point the sensor at the direction that provides the maximum amount of information to narrow down the uncertainty, whereas the MPSA approach prefers to continue pointing the sensor at the most probable direction. Based on the selected parameters, for an individual Monte Carlo sample, the MPSA and KLSA approaches are equivalent up to when the maximum W_{it} among all action candidates reaches $W^* = 0.5$. Therefore, over the Monte Carlo samples, the behaviors of the two algorithms initially share a similar evolution trend of $P[\text{object}]$, but diverge as the probability increases toward and exceeds 0.5. The focus of this Note is on the early stage of the search and it is demonstrated that the MPSA and KLSA approaches show a similar performance at this early stage. Note that, in Fig. 2, $P[\text{object}]$ is not strictly increasing over observations even for the MPSA case; this is because we constrain our sensor steering directions to be one of the particles although the true object is not necessarily one of them, which therefore causes the variation of the maximum $P[\text{object}]$ depending on the relative locations of the sensor, object, and particles over the orbit. This issue can be mitigated by resampling the particles or candidate steering directions (e.g., using a regularized particle filter).

To analyze the performance of the KLSA approach further, Fig. 3 shows the mean posterior entropy for the MPSA and KLSA approaches, averaged over the Monte Carlo simulations. Here, the posterior entropy is used as a measure of uncertainty. Again, during the initial observations, the entropy follows a similar trend for the KLSA and MPSA. However, during the later stages of the search, the information-theoretic KLSA reduces the entropy (i.e., reduces the uncertainty) more quickly than the MPSA, because it points sensor at the directions that provide us with the maximum amount of information.

Table 1 Simulation Settings.

| Parameter | Values |
|--|--------------------------------|
| Candidate and Object Initial Position Mean | [5715.1, 3325, 0] km |
| Candidate and Object Initial Velocity Mean | [-3.4352, 5.95, 3.9666] km/s |
| Candidate and Object Initial Position Variance | [50, 50, 50] km |
| Candidate and Object Initial Velocity Variance | [1E-4, 1E-4, 1E-4] km/s |
| Observer Initial Position | [6062.2, 3500, 0] km |
| Observer Initial Velocity | [-3.2675, 5.6595, 3.7730] km/s |
| Number of Candidate Orbits | 100 |
| Number of Observation Measurements | 20 |
| Time between Observation Measurements | 100 seconds |
| Number of Monte Carlo Trials | 400 |
| Field of View | 5 degrees |
| p_{DP} | 0.9 |
| p_{NA} | 0.9 |

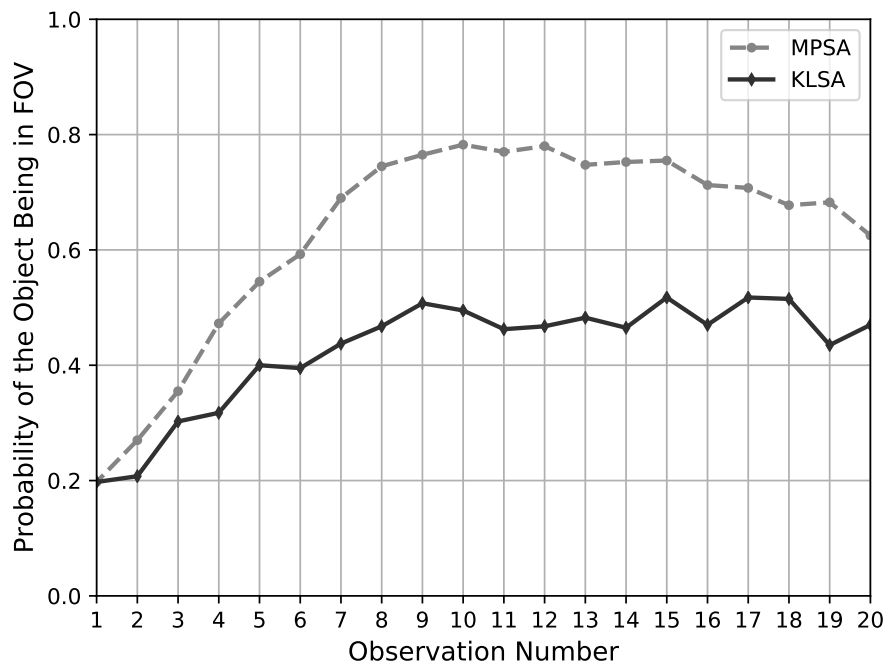


Fig. 2 Probability of the object being in the FOV for the Maximum Probability Search Algorithm (MPSE) and Kullback-Liebler Search Algorithm (KLSA). Results correspond to the problem definition given in Table 1.

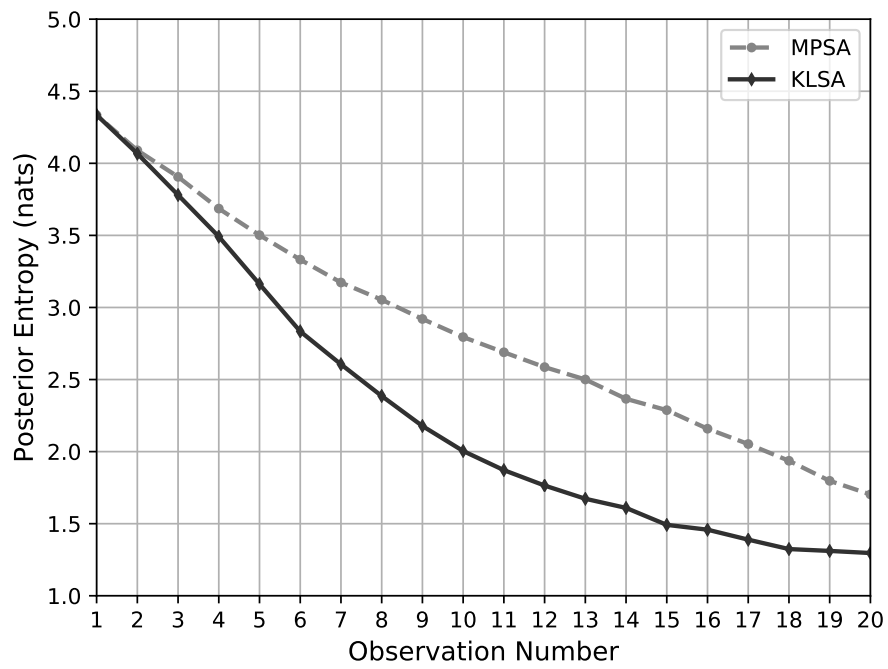


Fig. 3 Mean posterior entropy for the Maximum Probability Search Algorithm (MPSE) and Kullback-Liebler Search Algorithm (KLSA). Results correspond to the problem definition given in Table 1. The units for the entropy is natural unit (nats), i.e. $\sum_j -w^j \ln w^j$.

VI. Conclusion

This work analytically and systematically relates the Maximum Probability Search Algorithm (MPSA) and the Kullback-Liebler Search Algorithm (KLSA) for initial sensor search. Our mathematical analysis derived the expressions that govern the relationship between the directions that the MPSA would point the sensor at and those that the KLSA would point the sensor at, as well as deriving the condition under which these directions are equivalent. The equivalency of the MPSA and the KLSA under the derived condition is significant due to the lower computational cost of the MPSA, which helps support the possibility of autonomous onboard implementation. We also run simulations to show the numerical performance of the proposed sensor steering approaches. We believe that this Note provides the foundation for further sensor tasking method development, particularly regarding the role of the information-theoretic approach with respect to the maximum-probability approach. Combination of the search problem where information is gained from no-detection measurements with the global SSA problem where multiple sensors are tasked to observe multiple objects could be considered. Additionally, whereas the MPSA and KLSA have here been compared under a greedy or myopic search, comparison of the algorithms when optimizing over a time horizon could be considered.

References

- [1] National Research Council, *Continuing Kepler's Quest: Assessing Air Force Space Command's Astrodynamics Standards*, National Academies Press, 2012. <https://doi.org/10.17226/13456>.
- [2] Erwin, R., Albuquerque, P., Jayaweera, S., and Hussein, I., "Dynamic sensor tasking for Space Situational Awareness," Baltimore, MD, 2010, pp. 1153–1158. <https://doi.org/10.1109/ACC.2010.5530989>.
- [3] Sunberg, Z., Chakravorty, S., and Erwin, R. S., "Information Space Receding Horizon Control for Multisensor Tasking Problems," *IEEE Transactions on Cybernetics*, Vol. 46, No. 6, 2016, pp. 1325–1336. <https://doi.org/10.1109/TCYB.2015.2445744>.
- [4] Hussein, I. I., Jah, M. K., and Erwin, R. S., "An AEGIS-FISST Sensor Management Approach for Joint Detection and Tracking in SSA," *AAS/AIAA Space Flight Mechanics Meeting*, Kuai, HI, 2013.
- [5] DeMars, K. J., Hussein, I. I., Frueh, C., Jah, M. K., and Erwin, R., "Multiple-Object Space Surveillance Tracking Using Finite-Set Statistics," *Journal of Guidance, Control, and Dynamics*, Vol. 38, No. 9, 2015, pp. 1741–1756. <https://doi.org/10.2514/1.G000987>.
- [6] Williams, P. S., Spencer, D. B., and Erwin, R. S., "Coupling of Estimation and Sensor Tasking Applied to Satellite Tracking," *Journal of Guidance, Control, and Dynamics*, Vol. 36, No. 4, 2013, pp. 993–1007. <https://doi.org/10.2514/1.59361>.
- [7] Hussein, I. I., Sunberg, Z., Chakravorty, S., Jah, M. K., and Erwin, R., "Stochastic Optimization for Sensor Allocation Using AEGIS-FISST," *AAS/AIAA Space Flight Mechanics Conference*, Santa Fe, NM, 2014.
- [8] Nagavenkat, A., Singla, P., and Majji, M., "Mutual Information Based Sensor Tasking with Applications to Space Situational Awareness," *Journal of Guidance, Control, and Dynamics*, ????. To appear.

- [9] Murphy, T. S., and Holzinger, M. J., “Generalized Minimum-Time Follow-up Approaches Applied to Tasking Electro-Optical Sensor Tasking,” *Proceedings of the Advanced Maui Optical and Space Surveillance (AMOS) Technologies Conference*, 2017. URL <http://adsabs.harvard.edu/abs/2017amos.confE..54M>.
- [10] Schlenker, L., Sinclair, A. J., and Linares, R., “Angles-Only Orbit Determination Using Hamiltonian Monte Carlo,” *AIAA/AAS Space Flight Mechanics Meeting*, Kissimmee, FL, 2018. <https://doi.org/10.2514/6.2018-1975>.
- [11] Hobson, T., Gordon, N., Clarkson, I., Rutten, M., and Bessell, T., “Dynamic Steering for Improved Sensor Autonomy and Catalogue Maintenance,” *Proceedings of the Advanced Maui Optical and Space Surveillance Technologies Conference*, 2015.
- [12] Patel, H., Lovell, T. A., Russell, R., and Sinclair, A., “Relative Navigation for Satellites in Close Proximity Using Angles-Only Observations,” *AAS/AIAA Space Flight Mechanics Meeting*, Charleston, SC, 2012.
- [13] Woffinden, D. C., and Geller, D. K., “Observability Criteria for Angles-Only Navigation,” *IEEE Transactions on Aerospace and Electronic Systems*, Vol. 45, No. 3, 2009, pp. 1194–1208. <https://doi.org/10.1109/TAES.2009.5259193>.
- [14] Sherrill, R. E., Sinclair, A. J., and Lovell, T. A., “Virtual-Chief Generalization of Hill–Clohessy–Wiltshire to Elliptic Orbits,” *Journal of Guidance, Control, and Dynamics*, Vol. 38, No. 3, 2015, pp. 523–528. <https://doi.org/10.2514/1.G000110>.
- [15] Hobson, T. A., and Clarkson, I. V. L., “A Particle-Based Search Strategy for Improved Space Situational Awareness,” *Asilomar Conference on Signals, Systems and Computers*, Pacific Grove, CA, 2013, pp. 898–902. <https://doi.org/10.1109/ACSSC.2013.6810418>.
- [16] Hobson, T. A., and Clarkson, I. V. L., “An Experimental Implementation of a Particle-Based Dynamic Sensor Steering Method for Tracking and Searching for Space Objects,” *IEEE International Conference on Acoustics, Speech, and Signal Processing*, Florence, Italy, 2014, pp. 8018–8022. <https://doi.org/10.1109/ICASSP.2014.6855162>.
- [17] Patel, M., Sinclair, A. J., and Ho, K., “Information-Theoretic Target Search for Space Situational Awareness,” *AIAA/AAS Space Flight Mechanics Meeting*, Kissimmee, FL, 2018. <https://doi.org/10.2514/6.2018-0725>.
- [18] Patel, M., Sinclair, A. J., Yeong, H. C., Beeson, R., and Ho, K., “Dynamic Sensor Steering for Target Search for Space Situational Awareness,” *AAS/AIAA Astrodynamics Specialist Conference*, Snowbird, UT, 2018.
- [19] Beeson, R., Tomita, K., Gunasekara, O., Sinclair, A. J., and Ho, K., “Space-Based Target Search Methods using an Optical Sensor Model for Space Situational Awareness,” *AAS/AIAA Astrodynamics Specialist Conference*, Portland, ME, 2019.